

Fabrication of Submicrometer-Sized Gold Electrodes of Controlled Geometry for Scanning Electrochemical-Atomic Force Microscopy

Jeremy Abbou, Christophe Demaille,* Michel Druet, and Jacques Moiroux

Laboratoire d'Electrochimie Moléculaire, Unité Mixte de Recherche Université-CNRS 7591, Université de Paris 7-Denis Diderot, 2 place Jussieu, 75251 Paris Cedex 05, France

A method for fabricating submicrometer-sized gold electrodes of conical or spherical geometry is described. By generating an electric arc between an etched gold micro-wire and a tungsten counter electrode, the very end of the gold microwire can be melted and given an overall spherical or conical shape a few hundred nanometers in size. The whole wire is subsequently insulated via the cathodic deposition of electrophoretic paint. By applying a high-voltage pulse to the microwire, the film covering its very end can then be selectively removed, thus exposing a submicrometer-sized electrode surface of predefined geometry. The selective exposure of the preformed end of the microwire is demonstrated by cyclic voltammetry, scanning electron microscopy, and metal electrodeposition experiments. The electrophoretic paint coating provides a low-capacitance, robust insulating film allowing exploration of a very wide potential window in aqueous solution. The submicrometer-sized electrodes can easily be turned into probes suitable for combined scanning electrochemical-atomic force microscopy by bending and flattening the gold microwire so that the tip is borne by a flexible enough arm. The good agreement between theoretical and experimental scanning electrochemical microscopy approach curves thus obtained confirms that only the very end of the tip, of predefined geometry, is exposed to the solution.

The development of reliable techniques for the fabrication of submicrometer-sized electrodes is a subject of current interest largely driven by the much sought increase of resolution of the scanning electrochemical microscope (SECM).^{1,2} In this latter technique, a microelectrode is used to probe the local electrochemical reactivity of a surface. The spatial resolution of SECM is governed by the size of the microelectrode and has been so far mostly restricted to the micrometer range, as a result of the limited

availability of smaller microelectrodes. Any increase in resolution of SECM therefore relies on the development of new probes having a size significantly smaller than 1 μm . However, the fabrication and even more the characterization of submicrometer-sized electrodes have proved to be difficult. The main source of ambiguity results from the fact that, even when examined by scanning electron microscopy (SEM), the actual electroactive surface of submicrometer-sized electrodes is often difficult to resolve from the surrounding insulating sheath. However, for an electrode to be used as a SECM probe, its geometry must be perfectly known especially if any meaningful quantitative measurements are to be made with it.^{3–5} The development of techniques aimed at fabricating submicrometer-sized electrodes of highly characterized geometry and suitable as tips for SECM is therefore very desirable.

The final shape of the electrode itself is typically imposed by the fabrication process, and in the range of submicrometer-sized electrodes suitable for SECM, the electrode shapes produced so far seem to have been limited to disks or cones.^{2c} Although very attractive, tips of spherical geometry have been so far restricted to the micrometer range.⁶

Disk-in-glass electrodes of a few tens of nanometers in diameter have been obtained by pulling metal wires embedded within glass capillaries and thoroughly characterized.⁷ Once polished, the electrode surface presented the geometry of a disk slightly protruding from a large surrounding glass sheath.

However, most of the SECM-compatible submicrometer-sized electrodes are conical as they are made starting from etched metal microwires. Electrochemical etching of metal microwires, implying anodic dissolution of the end of the microwire, gives the extremity of the microwire a tapered shape. Making a microelectrode out of such an etched wire involves the insulation of the whole of the wire surface but its very end. To achieve this goal, insulation

* Corresponding author. E-mail: demaille@paris7.jussieu.fr.

- (1) Bard, A. J.; Fan, F.-R. F.; Mirkin, M. V. In *Electroanalytical Chemistry*; Bard, A. J., Ed.; Marcel Dekker: New York, 1994; Vol. 18, p 243.
- (2) (a) *Scanning Electrochemical Microscopy*; Bard, A. J., Mirkin, M. V., Eds.; Marcel Dekker: New York, 2001. (b) Bard, A. J. In *Scanning Electrochemical Microscopy*; Bard, A. J., Mirkin, M. V., Eds.; Marcel Dekker: New York, 2001 pp 636–637. (c) Fan, F.-R. F.; Demaille, C. In *Scanning Electrochemical Microscopy*; Bard, A. J., Mirkin, M. V., Eds.; Marcel Dekker: New York, 2001; pp 75–107.

- (3) (a) Baranski, A. S. *J. Electroanal. Chem.* **1991**, 307, 287–292. (b) Oldham, K. B. *Anal. Chem.* **1992**, 64, 646–651.

- (4) Mirkin, M. V.; Fan, F.-R. F.; Bard, A. J. *J. Electroanal. Chem.* **1992**, 328, 47–62.

- (5) (a) Fulian, Q.; Fisher, A. C.; Denuault, G. *J. Phys. Chem. B* **1999**, 103, 4387–4392. (b) Fulian, Q.; Fisher, A. C.; Denuault, G. *J. Phys. Chem. B* **1999**, 103, 4393–4398.

- (6) Demaille, C.; Brust, M.; Tsionsky, M.; Bard, A. J. *Anal. Chem.* **1997**, 69, 2323–2328.

- (7) (a) Shao, Y.; Mirkin, M. V.; Fish, G.; Kokotov, S.; Palanker, D.; Lewis, A. *Anal. Chem.* **1997**, 69, 1627–1634. (b) Ballesteros, B.; Schuhmann, W. *Electroanalysis* **2002**, 14, 22–28.

techniques reported so far fall in two categories: one-step processes that avoid to coat the extremity of the tip, and two-step processes that consist of completely coating the wire and then selectively uncovering the tip end. In a typical one-step insulation process, an etched wire is translated through a bed of molten insulating material such as glass,^{8a} polymer,^{8b} or wax,⁴ and the sharp end of the wire, which naturally tends not to be wetted by the molten material, remains hopefully uncoated. Even though electrodes of nanometric dimensions could be produced in this way,^{8b} it has been shown that one-step insulation processes often result in recessed electrodes, the apparent electrochemical size of which being solely related to the dimension of the "hole" left in the coating film at the extremity of the electrode.³ In two-step insulation processes, the complete coating of the wire by the insulating film has to be followed by a second step aimed at selectively exposing the tip end. Typically, this second step is thermal curing during which the film is expected to shrink,⁹ but chemical dissolution of the coating, hopefully occurring at the tip end, is also sometimes required.¹⁰ In every case, although the exposing step is most important, as it ultimately defines the true electrode surface, it somehow often relies on the "good will" of the coating material.

The use of anodic electrophoretic paint as a microelectrode coating material was introduced some time ago.¹¹ More recently, the electrophoretic deposition of anodic paint onto etched platinum wires, followed by thermal curing of the film, was shown to produce micrometer-sized conical electrodes.⁹ Electrodes of smaller apparent dimensions, down to a few nanometers, as characterized by cyclic voltammetry, could be produced using the same technique but only by repeated deposition/curing cycles.^{9,12} However, it was shown that the smallest electrodes produced this way were most likely recessed.⁹ In an attempt to make smaller electrodes in a single deposition step, use of the newer generation of cathodic electrodeposition paints has been reported.¹³ These cathodically deposited paints are formulated to be less prone to shrink during thermal curing.¹⁴ They thus allow production of smaller tips in a single deposition step but often result in the complete and irreversible insulation of the whole electrode. To circumvent that problem, an "inverted deposition" technique, involving bending the tip so that its very end just breaks through the surface of the electrophoretic paint solution, was applied to the making of etched carbon fiber microelectrodes.¹⁵ Yet, even in this case, several cycles of deposition/curing steps were required and this method probably also leads to recessed electrodes. Thus, to date, exposing convincingly the very end of a submicrometer electrode made from an etched wire remains a challenge.

Unrelated to the difficulty of making efficient microelectrode probes, high-resolution imaging by SECM requires the combination of SECM with a near-field technique adapted to the exploration of nanometric spaces.^{2b} In such a combined configuration, the near-field technique provides a feedback mechanism allowing precise control of the tip-surface separation while the local electrochemical surface reactivity is independently probed. Systems based on shear force feedback¹⁶ or built around an atomic force microscope (AFM) have been described.¹⁷ Combined AFM/SECM probes were constructed either from etched platinum wires that were insulated by the deposition of anodic electrophoretic paint^{17a,b} or by integrating a microelectrode in a standard AFM tip using focused ion beam technique.^{17c}

The aim of the present work was to construct gold electrodes of submicrometer dimension, of well-defined geometry, presenting a clear and clean electroactive surface and that could ultimately be used as combined AFM/SECM probes.

A novel method to form conical or spherical structures of down to a few hundred nanometers in size at the very end of gold microwires is reported. These structures are created by taking advantage of the localized melting of the extremity of gold microwires triggered by an electric discharge. The electric arc is provoked by applying a potential of a few kilovolts to a sharpened tungsten wire facing the etched gold microwire. The intensity of the discharge, and thus the size and shape of the structure formed at the extremity of the gold microwire, can be controlled by adjusting the parameters of the homemade spark generator setup. The whole gold wire is then insulated by electrodeposition of a cathodic electrophoretic paint. The problem of exposing selectively the preformed extremity of the electrode is then solved in an original way. It is demonstrated here that complete and selective exposure of the preformed electrode surface can be achieved simply by applying a voltage pulse of a few kilovolts amplitude to the painted microwire. The resulting intense electric field localized at the tip end is then strong enough to uncover the preformed structure. The spherical or conical submicrometer-sized electrodes constructed by the above technique are shown to have a good voltametric behavior consistent with their size. In particular, the potential window in aqueous solution is very large. When the same tip-making technique is carried out starting from etched, bent, and flattened wires, it yields combined submicrometer-sized AFM/SECM probes of spherical geometry. The defined geometry of the electrode probe is reflected by the very good agreement between the experimental SECM approach curves and the theoretical one, calculated for the appropriate geometry.

EXPERIMENTAL SECTION

Cyclic Voltammetry and AFM/SECM Apparatus. Cyclic voltammetry experiments were performed with a three-electrode setup up using a platinum wire and a KCL saturated calomel

- (8) (a) Penner, R. M.; Heben, M. J.; Lewis, N. S. *Anal. Chem.* **1989**, *61*, 1630–1636. (b) Penner, R. M.; Heben, M. J.; Longin, T. L.; Lewis, N. S. *Science* **1990**, *250*, 1118–1121.
- (9) Slevin, C. J.; Gray, N. J.; Macpherson, J. V.; Webb, M. A.; Unwin, P. R. *Electrochem. Commun.* **1999**, *1*, 282–288.
- (10) Sun, P.; Zhang, Z.; Guo, J.; Shao, Y. *Anal. Chem.* **2001**, *73*, 5346–5351.
- (11) (a) Bach, C. E.; Nichols, R. J.; Beckmann, W.; Meyer, H.; Schulte, A.; Bensenhard, J. O.; Jannakoudakis, P. D. *J. Electrochem. Soc.* **1993**, *140*, 1281–1284. (b) Schulte, A.; Chow, R. H. *Anal. Chem.* **1996**, *68*, 3054. (c) Schulte, A.; Chow, R. H. *Anal. Chem.* **1998**, *70*, 985–990.
- (12) Conyers, J. L.; White, H. S. *Anal. Chem.* **2000**, *72*, 4441–4446.
- (13) Gray, N. J.; Unwin, P. R. *Analyst* **2000**, *125*, 889–893.
- (14) Ricard, R. BASF coatings, personal communication, 2002.
- (15) Kucernak, A.; Chen, S. *Electrochem. Commun.* **2002**, *4*, 80–85.

- (16) (a) James, P. I.; Garfias-Mesias, L. F.; Moyer, P. J.; Smyrl, W. H. *J. Electrochem. Soc.* **1998**, *145*, L64–L66. (b) Büchler, M.; Kelley, S. C.; Smyrl, W. H. *Electrochem. Solid State Lett.* **2000**, *3*, 35–38. (c) Ludwig, M.; Kranz, C.; Schuhmann, W.; Gaub, H. E. *Rev. Sci. Instrum.* **1995**, *66*, 2857–2860. (d) Hengstenberg, A.; Kranz, C.; Schuhmann, W. *Chem. Eur. J.* **2000**, *6*, 1547–1554.
- (17) (a) Macpherson, J. V.; Unwin, P. R. *Anal. Chem.* **2000**, *72*, 276–285. (b) Macpherson, J. V.; Webb, M. A.; Unwin, P. R. *Anal. Chem.* **2001**, *73*, 550–557. (c) Kranz, C.; Friedbacher, G.; Mizaikoff, B.; Lugstein, A.; Smoliner, J.; Bertagnolli, E. *Anal. Chem.* **2001**, *73*, 2491–2500.

electrode as, respectively, the counter and reference electrodes. The apparatus was composed of a function generator (EG&G PARC model 175), a homemade potentiostat,¹⁸ and a low-current electrometer (Keithley 617).

The AFM/SECM experiments were carried out with a Molecular Imaging PicoSPM AFM microscope (acquired from Sci-entec) that was equipped with a fluid cell. Both the counter and quasi-reference electrodes (QRE) were platinum wires, immersed in the fluid cell. A homemade bipotentiostat allowed the measurement of the probe current and provided an independent control of the electrochemical potential of the tip and of the substrate. The Molecular Imaging Picoscan controller was used to generate the potential applied to the tip by the bipotentiostat and to acquire the tip current data. For recording of the AFM/SECM approach curves, the tip movement and potential were controlled via a homemade script program. When the tip approached a conducting substrate, the program could be used to prevent the tip–surface short circuit to occur by opening the tip circuit when an abrupt variation of the deflection, indicative of a tip–surface contact, was detected. When such a protecting software mechanism was disabled, a short circuit was detected indicating that no residual insulating film was present at the tip surface. In some cases, however, the loss of such ohmic contact between the tip and substrate was observed during the AFM/SECM experiment, probably as a result of tip contamination.¹⁹ The contact was restored after the tip was cleaned by cycling in a 1 N H₂SO₄ solution at a scan rate of 1 V/s.²⁰ During the measurements, the microscope head was placed inside a homemade vibration-proof Faraday cage. The conductive substrate was made of a few-micrometer-thick gold film evaporated onto a bare microscope slide. Just before use, the backside of the gold film was glued onto a another glass slide using a cyanoacrylate-based glue and peeled using a razor blade. The working surface was therefore the gold surface initially facing the slide onto which gold had been evaporated. AFM characterization showed that the average roughness of such a surface was of a few tens of nanometers.

Single High-Voltage Pulse Generator. *Schematics of the Electronic Circuit.* The schematics of the homemade high-voltage pulse generator used in the present work are reported in Figure 1a. The electronic circuit was designed so that a single high-voltage pulse was generated at its negative output pole. When triggered, the upper part of the circuit supplied the lower left part with ~ 5 V for 30 ms. During this time interval, the circuit around the BC337 transistor charged the 0.47- μ F capacitor up to a voltage of 200 V. At that stage, firing of the thyristor caused an abrupt discharge of the capacitor into the high-voltage transformer. This resulted in a short (~ 1 μ s) single high-voltage pulse at the negative output pole of the circuit. High-voltage peaks of an amplitude as high as 6 kV could be generated.

Tip Holding Stage and Positioning Setup. The homemade tip holding stage and the positioning setup shown in Figure 1b was used both for the spark-induced tip end remodeling experiments and for the exposure of the painted tips. The tungsten wire, used

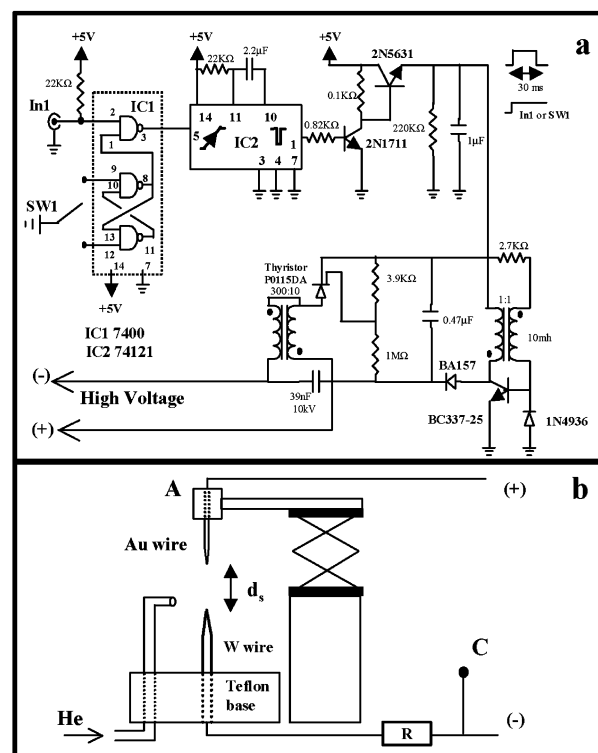


Figure 1. Schematic diagram of the high-voltage single pulse/spark generator setup. (a) Schematics of the electronic circuit of the high-voltage single pulse generator. (b) Diagram of the positioning setup. The configuration shown is the closed-circuit configuration used to preform submicrometer-sized structures at the end of etched gold wires by arc discharge (see text).

as the cathode, was held in a gator clip inserted in a hole drilled in the center of a Teflon base and was electrically connected to the high-voltage (negative) output pole of the pulse generator. The gold wire, used as the anode, was held in a small gator clip that was mounted between the rubber-coated jaws of a clamp. That clamp was used as the arm of a coarse positioning system constructed from a microjack. When required, the gold wire could be connected to the positive pole of the generator in (A). A vernier microscope was used to measure the interelectrode distance d_s that could be set with an accuracy of ± 0.2 mm. A resistance R (1 kΩ–1 MΩ) was inserted in the circuit as shown in Figure 1b, so that it could be physically changed at will. A small plastic nozzle, placed a few millimeters away from the electrodes and pointing at the interelectrode gap, was positioned on the Teflon base in order to blow helium between the electrodes.

Scanning Electron Microscopy. The images were acquired using a LEO S440 scanning electron microscope at an electron beam energy of 20 keV. The painted wires and electrodes were imaged as is; that is, they were not coated with a thin metal-sputtered layer.

Materials. 1,1'-Ferrocenedimethanol (98%) was purchased from Aldrich. All the other chemicals were purchased from Prolabo and used as received. The cathodic electrophoretic paint (BASF FT83-0250) was a gift from BASF coatings. All aqueous solutions were prepared with Milli-Q purified water (Millipore). The gold microwires, 60- μ m diameter (99.99%), were purchased from Good Fellow.

(18) Garreau, D.; Savéant, J. M. *J. Electroanal. Chem.* **1972**, *35*, 309–331.

(19) (a) O'Shea, S. J.; Atta, R. M.; Welland, M. E. *Rev. Sci. Instrum.* **1995**, *66*, 2508–2512. (b) Lantz, M. A.; O'Shea, S. J.; Welland, M. E. *Phys. Rev. B* **1997**, *56*, 15345–15352. (c) Salmeron, M.; Neubaueur, G.; Folch, A.; Tomitori, M.; Ogletree, D. F.; Sautet, P. *Langmuir* **1993**, *9*, 3600–3611.

(20) Rand, D. A. J.; Woods, R. J. *J. Electroanal. Chem.* **1972**, *35*, 209–218.

Electrochemical Etching of Gold Microwires. The technique used to etch the gold microwire was adapted from the literature.²¹ Briefly, the last millimeter of the wire was immersed in a solution containing 10 mL of saturated CaCl_2 , 40 mL of Milli-Q water, and 5 mL of ethanol. Ethanol was added in order to reduce the size of the bubbles formed at the gold wire during etching. A potential of +7 V was applied between the gold wire (anode) and a large platinum foil (cathode). The etching was complete in ~ 2 min when the extremity of the etched wire was no longer in contact with the solution. This gave the extremity of the gold wire a conical aspect with a taper length ranging from 150 to 250 μm and a characteristic rounded tip end.

Remodeling of the Etched Wire End by Arc Discharge-Induced Melting. The homemade high-voltage pulse generator reported in Figure 1 was used to generate the spark required to melt the end of the etched wires. The cathode was a 0.25-mm-diameter tungsten wire electrochemically etched to a fine point using reported techniques.²² The etched gold wire was the anode of the setup. In the closed-circuit configuration, the gold wire was connected to the positive pole of the high-voltage generator. Whereas, in the open-circuit configuration, the gold wire was disconnected from the positive pole of the high-voltage generator in point A (Figure 1b). To generate the spark in a helium atmosphere, a gentle helium flow was blown toward the inter-electrode gap. When the setup was suitably configured (see text), the success yield for forming conical structures was 50% (the other 50% of the structures formed were spheres). The success yield for forming spheres was 100%. In any case, the size dispersion was $\pm 50\%$.

It is worth reporting that spark experiments directly starting from etched painted wires were also carried out. However, in this case, both the air and the *film* breakdown potential had to be reached before a spark was generated. Consequently, the voltage required was very high and as a result no gold spheres smaller than $\sim 10 \mu\text{m}$ in size could be formed this way.

Insulation of the Submicroelectrodes by Deposition of Cathodic Electrophoretic Paint. The paint solution was diluted in a 1:1 (v:v) ratio with a 3 mM acetic acid aqueous solution. The wire to be painted was first thoroughly rinsed sequentially with water, acetone, and dichloromethane before being immersed into the paint solution. The electrochemical set up was used in a two-electrode configuration, the gold wire being the cathode and a platinum coil the anode. The film deposition was triggered by scanning the electrode potential from 0 to -5 V at 50 mV/s . The electrode was then disconnected, removed from the paint solution, and gently rinsed with water. The deposited paint film was then allowed to cure in an oven at 180°C for 20 min. We observed that over 80% of the wires were perfectly insulated at this stage.

Selective Exposure of the Preformed Tip by Applying a High-Voltage Pulse. The apparatus reported in Figure 1 was also used to generate the high-voltage pulse required to selectively expose the preformed tips once they were painted. The submicroelectrode to be exposed was connected in parallel to the spark-producing circuit in point C (Figure 1b), and the resistance R was

short circuited. For these experiments, the anode of the spark circuit was a plain $60\text{-}\mu\text{m}$ gold wire while the cathode was a tungsten wire. When the apparatus was triggered, the cathode voltage raised very abruptly until a spark was generated between the tungsten and the gold wires. In this configuration, no spark was generated at the electrode to expose but it experienced the same high-voltage pulse as the cathode did, the occurrence of the spark limiting the pulse amplitude. The highest voltage reached by the electrode to be exposed could thus be controlled by adjusting the distance d_s separating the spark-producing wires. The values of d_s typically used for the exposure ranged from 0.5 to 2 mm. Assuming a breakdown field of air of $3 \times 10^6 \text{ V/m}$,^{23a} that translated into an applied voltage peak between the wires in the 1.5–6-kV range. The preformed tips could be equivalently exposed by applying either several voltage pulses at the lowest voltage or a single pulse at the highest voltage. The exposure yield was 100% (no tips remained insulated after the high-voltage pulse treatment).

Making Combined AFM/SECM Probes from Spherical Submicroelectrodes. The technique used to convert the submicroelectrodes into combined AFM/SECM probes was adapted from the literature.^{17a} The starting gold microwire was bent at a right angle a few hundred micrometers before its end. The bent portion of the microwire was then flattened by pressing it between two polished inox plates placed in a bench vice. After that, the end of the other portion of the wire was etched as described above. The wire was then mounted onto the homemade spark generator, and the desired shape was given to the tip end. For the AFM/SECM experiments reported here, spherical tip shapes were preferred. The flattened gold wire, bearing the preformed structure at its end, was then insulated by deposition of cathodic electrophoretic paint as described above. The tip was subsequently glued onto a conventional AFM silicon nitride ship and stored as is. The preformed tip end was exposed by the high-voltage pulse technique reported above shortly before the tip was used. The spherical shape of the tip end was confirmed by visual examination using an optical microscope. Its size was derived from cyclic voltammetry experiments.

Iron Electrodeposition onto the Submicrometer-Sized Electrodes. Iron was electrodeposited onto freshly exposed electrodes by reduction of Fe^{2+} ions from a 1 mM FeSO_4 solution. This solution also contained 0.1 M Na_2SO_4 as a supporting electrolyte and was acidified by 1 mM H_2SO_4 . The potential of the electrode was scanned from -0.3 to -1.5 V versus SCE and held there for a few seconds. The tip was then disconnected, rinsed with water, and ready for SEM imaging. Control experiments in which the tip potential was scanned back to -0.3 V showed a sharp voltametric peak corresponding to the stripping of the iron deposit.

RESULTS AND DISCUSSION

Production of Submicrometer-Sized Gold Structures with a Conical or Spherical Geometry by Generating an Arc Discharge at Etched Gold Microwires. We propose here a novel technique aimed at remodeling the very end of etched gold microwires in order to form submicrometer-sized structures of

(21) (a) Sørensen, A. H.; Hvid, U.; Mortensen, M. W.; Mørch, K. A. *Rev. Sci. Instrum.* **1999**, *70*, 3059–3067. (b) Nam, A. J.; Teren, A.; Lusby, T. A.; Melmed, A. J. *J. Vac. Sci. Technol. B* **1995**, *13*, 1556–1559.

(22) Kerfriden, S.; Nahlé, A. H.; Campbell, S. A.; Walsh, F. C.; Smith, J. R. *Electrochim. Acta* **1998**, *43*, 1939–1944.

(23) (a) Jonassen, N. In *Electrostatics*; Jonassen, N., Ed.; Chapman & Hall: New York, 1998; p 26 (b) *Ibid*; p 42.

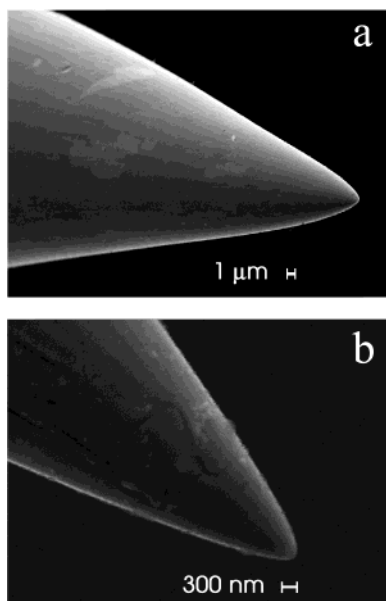


Figure 2. SEM micrographs showing (a) the extremity of a bare etched gold microwire and (b) the extremity of an etched microwire insulated by a film of reticulated electrophoretic cathodic paint and subsequently "exposed" by the high-voltage pulse technique to an apparent electrochemical size of 1 μm .

controlled geometry that can ultimately be used as submicroelectrodes. The reported technique is inspired from the "ball-bonding" process routinely employed by the microelectronics industry as a means of interconnecting chips and output pins.²⁴ It consists of taking advantage of the localized melting of the very end of gold wires triggered by an electric discharge. In a typical configuration, a tension of a few kilovolts is applied between a gold microwire and a tungsten cathode, thus provoking an arc discharge. The locally generated heat is sufficient to melt the extremity of the gold microwire that balls up before solidification occurs. The ball diameter is typically a few times as large as the supporting wire diameter. Transposing this process to the formation of submicrometer-sized structures implies first that the diameter of the starting wire has to be decreased by electrochemical etching, so that its very end is reduced to a size of a few tens of nanometers. Second, the energy produced by the arc discharge, which ultimately governs the size of the structure formed at the end of the etched wire, has to be finely controlled.

Etching of the starting microwire is carried out in a way adapted from the literature and is described in the Experimental Section. It results in giving the end of the microwire a tapered shape such as the one shown in the SEM image presented in Figure 2a.

The etched gold wire is then mounted as the anode of the homemade spark generator setup presented in Figure 1. This setup was constructed in order to gain some control over the energy of the discharge process. Its electronic circuit is designed to generate the single high-voltage pulse required to produce the spark. In a closed-circuit configuration, a sharp tungsten wire is connected to the high-voltage output of the pulse generator while the etched gold wire is connected to the low-voltage positive pole

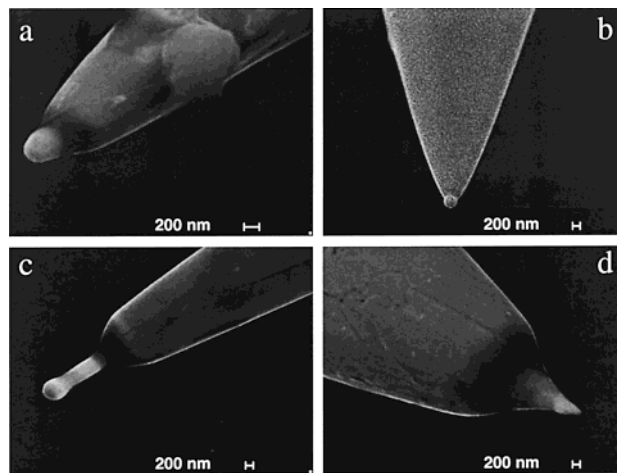


Figure 3. SEM micrographs of submicroelectrodes. The electrodes are made from gold wires bearing submicrometer-sized structures formed as a result of the controlled arc discharge technique reported in the text. The body of the wire is insulated by a layer of electrophoretic paint; only the preformed tip end is bare gold. Settings of the spark generator used to make the submicroelectrodes shown: (a) open-circuit configuration, $R = 0$, $d_s = 0.5$ mm, shielding gas is air; (b) open-circuit configuration, $R = 0$, $d_s = 0.5$ mm, shielding gas is helium; (c) open-circuit configuration, $R = 0$, $d_s = 1$ mm, shielding gas is air; (d) closed-circuit configuration, $R = 500$ k Ω , $d_s = 1$ mm, shielding gas is air.

of the generator. The overall intensity of the spark discharge can be controlled by varying the distance d_s between the wires, the resistance R in series with the cathode and the nature of the gas filling the interelectrode gap. By choosing the appropriate conditions, it is then possible to reproducibly form, at the end of etched wires, conical or spherical structures such as the ones seen on the SEM images presented in Figure 3. The exact settings leading to the different shapes are detailed in the corresponding caption and are discussed below.

Formation of Spherical Structures. In the closed-circuit configuration described above, the spark typically results in the formation of spherical structures at the end of the etched wire. The diameter of the spheres ranges from a few tens of micrometers down to 1 μm , depending on the conditions of their formation. As a rule, every change in the setting parameters of the spark generator that diminishes the energy transferred to the end of the wire results in a decrease of the ball size. Thus, increasing the current-limiting resistance R was found to decrease the diameter of the ball from ~ 10 μm (R of a few ohms) to a few micrometers (R of a few hundreds of kilohms). The distance between the electrodes d_s was found to have an even greater influence on the sphere diameter: when d_s is lowered, a lower voltage is required to provoke the electrical breakdown of the gas between the electrodes, and therefore, the resulting sphere diameter is smaller. However, even at the lowest controllable value of d_s that could be reliably set (0.5 mm) and for the highest resistance used (above which no spark is further produced: R of a few megaohms), no spheres smaller than 1–2 μm are formed in the closed-circuit configuration.

Smaller spheres can only be formed in an open-circuit configuration in which the gold wire is disconnected from the spark-producing circuit. This configuration limits the energy transferred to the wire, but even then is a clearly visible and audible spark

(24) Striny, K. M. In *VLSI Technology*, 2nd ed.; Sze, S. M., Ed.; McGraw-Hill: New York, 1988; Chapter 13, pp 589–594.

seen and heard, the charges thus transferred subsequently dissipating via decay through the air.^{23b} This open-circuit configuration leads to the formation, for an interelectrode spacing of 0.5 mm, of spherical or hemispherical structures of $\sim 0.5 \mu\text{m}$ in diameter, such as the one shown in Figure 3a.

Spheres of smaller diameter can be formed using the open-circuit configuration if the gas filling the gap between the electrodes is changed from air to helium. The nature of the shielding gas is indeed known to influence the formation of balls in the ball-bonding process as the thermal conductivity of the gas plays a central role in the amount of heat driven to the very end of the wire.²⁵ Helium has a thermal conductivity 6 times higher than that of air and is therefore a good candidate for the shielding gas. Using helium with the setup presented in Figure 1, in an open-circuit configuration and at an interelectrode spacing of 0.5 mm, leads to the formation of spherical structures, such as the one presented in Figure 3b, having diameters ranging from 300 to 150 nm.

Formation of Conical or Elongated Structures. The formation of elongated structures such as the one presented in Figure 3c, or roughly conical structures such as the one presented in Figure 3d, is also observed as a result of the spark discharge. The energy required to form such structures is clearly higher than the energy needed to form submicrometer-sized balls: they are formed in air, at greater interelectrode gap and, for the conical structures, in a closed-circuit configuration.

Insulation of Preformed Gold Tips by Deposition of Cathodic Electrophoretic Paint. Insulation of the gold wires bearing the preformed structure at their very end is then carried out via the deposition of a cathodic electrophoretic paint. This paint consists of a solution of charged micelles of NH_2 -bearing polymer chains suspended in an aqueous solution. The paint solution is kept acidic so that the amine groups remain protonated, which ensures the solubility of the micelles. To trigger the deposition of the film, the gold microwire bearing the preformed structure is immersed in the paint solution and its potential is scanned from 0 to -5 V at 50 mV/s . At such cathodic potentials, the protons are reduced and the ensuing local rise of pH triggers the precipitation of the deprotonated chains onto the wire surface. Electrophoretic deposition is followed by a thermal curing step during which the primary amines borne by the polymeric chains are allowed to react with diisocyanates also present in the paint composition. The resulting film is therefore highly cross-linked. This painting technique differs from what had already been reported in a previous work about microelectrode insulation using cathodic electrophoretic paints where the electrode potential was not scanned but stepped to negative values and held there for a few seconds.¹³ Experiments aimed at comparing both deposition techniques showed that scanning the electrode potential instead of stepping it resulted in better insulation of the electrode. Using an optical microscope, the freshly deposited film can clearly be seen all along the wire but it notably forms a bulb at $\sim 10 \mu\text{m}$ before the tip end. After thermal curing, that bulb disappears, indicating that the paint flows along the wire during curing as its viscosity decreases before reticulation starts.¹⁴

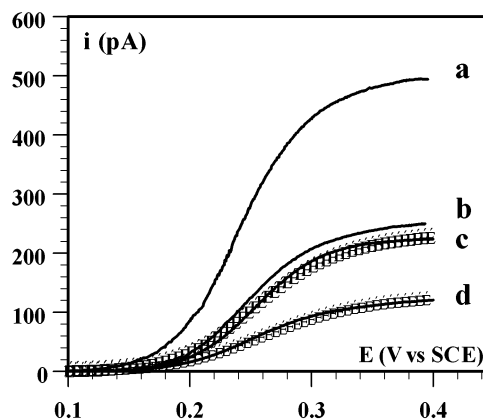
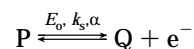


Figure 4. Cyclic voltammetry of ferrocenedimethanol at submicroelectrodes. The cyclic voltammograms (a–d) were recorded using the electrodes shown respectively in the SEM micrographs c, d, a, and b of Figure 3. The forward and backward traces are superimposed. From the value of the plateau current of the voltammograms (a–d), assuming a spherical geometry, the electrochemical radius of the electrodes are respectively estimated to be of 550, 300, 250, and 150 nm. The open circles correspond to the fitting of the whole voltammogram using eq 2. Ferrocenedimethanol is at a concentration of 1 mM in 0.1 M KH_2PO_4 , the scan rate is 20 mV/s , and the temperature is 25°C .

Selective Exposure of the Preformed Structures: Conical and Spherical Electrodes.

When the painted wires are characterized by cyclic voltammetry in an aqueous solution of 1 mM ferrocenedimethanol ($\text{Fc}(\text{diOH})$) in 0.1 M KH_2PO_4 , no matter the shape given to the preformed structure, no current signal is recorded. This result evidences that the painted wires are completely insulated by the electrophoretic cathodic paint, thus confirming the well-known high insulating power of these paints.^{13,15} The surface of the preformed structure is then selectively exposed in an original way by applying a voltage pulse of a few kilovolts amplitude to the painted wires, making use of the high-voltage setup (Figure 1). The electrode to be exposed is connected to the high-voltage output of the generator *in parallel* to a circuit composed of a plain gold wire facing a tungsten wire. When the generator is triggered, a spark is generated between these two wires and not at the surface of the insulated preformed wire, that thus only experiences a short high-voltage pulse (see Experimental Section for details). Nevertheless, after this pulse treatment, the tip electrode typically exhibits nicely S-shaped voltammograms as shown in Figure 4. This result shows that the transient high electric field created at the very end of the electrode uncovers it by locally blowing the film away.

The oxidation of the ferrocenedimethanol taking place at the microelectrode surface can be represented as



where P and Q respectively stand for the reduced and oxidized forms of the ferrocenedimethanol. E° is the standard potential of the redox couple, α the transfer coefficient (taken here as $\alpha = 0.5$), and k_s the rate constant of the heterogeneous electron transfer.

From the value of the limiting current i_∞ measured at the plateau of the sigmoid-shaped voltammogram, the apparent

(25) Onuki, J.; Koizumi, M.; Suzuki, H.; Araki, I.; Lizuka, T. *J. Appl. Phys.* **1990**, *68*, 5610–5614.

electrochemical size of the exposed area can be determined. Assuming the exposed surface is spherical, the plateau current is related, for a single-electron process, to the sphere radius a by²⁶

$$i_{\infty} = 4\pi FDC_p a \quad (1)$$

with F the Faraday constant, D the diffusion constant of $\text{Fc}^{\text{d}}\text{OH}$ ($D = 7.4 \times 10^{-6} \text{ cm}^2 \text{ s}^{-1}$ as measured below), and C_p its bulk concentration.

Electrochemical radii of 550, 280, 250, and 150 nm were respectively obtained from the voltammograms a–d presented in Figure 4.

These results indicate that the high-voltage pulse obviously removes some (small) portion of the film but it is still to be shown that the only uncovered and therefore electroactive part of the electrode is the preformed end of the gold tip.

The first evidence of this is given by the good correlation that was consistently observed between the electrochemical size of the tip determined as described above and the actual size of the preformed structure as measured by SEM. This can be seen for the tips giving rise to the voltammograms reported in Figure 4a–d as the SEM images of these very same tips are shown respectively in the parts c, d, a, and b of Figure 3. However, for the tips of elongated and conical geometry, the above correlation between the electrochemical and actual size of these tips can only be semiquantitative. It is more accurate for the more spherical tips imaged in Figure 3a,b and can be refined to yield a radius of 320 nm for the conical tip in Figure 3d, using the recently reported theoretical expression of the plateau current for such an electrode geometry.²⁷

Another evidence of the fact that the preformed tip is uncovered is brought to us by a careful examination of the SEM images of Figure 3. At least for the biggest electrodes, the very good contrast observed in SEM allows one to differentiate between the parts of the electrode still covered by the film and the ones exposed. The part covered by the film, which is most of the wire surface, appears to be dark and has a barklike aspect, showing numerous “veins”, whereas the preformed tip end appears to be very light and almost featureless. This light aspect compares well with the one of the bare (etched) gold wire presented in Figure 2a and strongly suggests that the preformed structures are indeed also bare. The observed material-dependent SEM contrast is made possible by the fact that the imaged electrodes are not coated with a thin metal-sputtered layer, as is usually the case for samples examined by SEM. Nevertheless, no electrostatic charging phenomenon is seen on the images, showing that the incident electron beam can penetrate the thin insulating film. As a result, the intensity of the secondary electron emission, used to construct the images, not only reflects the topography but is also modulated by the presence of the film.²⁸

Yet another, even more conclusive, evidence that the preformed end of the tip is the sole exposed part of the microelec-

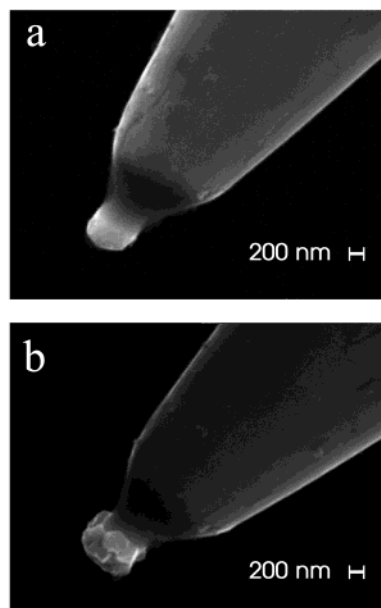


Figure 5. SEM micrographs of the submicrometer-sized gold electrode before (a) and after (b) the electrodeposition of iron from a 1 mM FeSO_4 solution. The crystal-shaped iron deposit visible in (b) grew exclusively onto the preformed tip end of the electrode, showing that it is indeed the only area exposed to the solution.

trode is brought by the metal electrodeposition experiment described below. In that experiment, a submicroelectrode is preformed, exposed, and tested as described above. After being imaged by SEM, iron is electrodeposited on the submicroelectrode by reduction of Fe^{2+} ions in an acidic solution as described in the Experimental Section. Comparison of the SEM images of the same tip taken before (Figure 5a) and after metal deposition (Figure 5b) shows that the iron growth (irregular crystals) occurred selectively at the very end of the tip, on the preformed structure and stops at the exact limit between the high and low SEM contrast part of the tip end.

This shows unambiguously that only the very end of the tip, corresponding to the preformed structure, is uncovered by the high-voltage pulse. Incidentally it also validates the identification of the film boundary based on SEM contrast.

The physical reason behind the remarkable selectivity of the high-voltage pulse technique for exposing the preformed structure is not absolutely clear. When applied to simply etched gold wires, bearing no preformed structure at their extremity, this same exposing technique yields ambiguous results: tips can be apparently exposed as judged from their cyclic voltammogram, but their SEM image shows no clear candidate for the actual electrode surface. This is illustrated by the SEM image presented in Figure 2b that shows a non-preformed (simply etched) painted and exposed electrode that has an electrochemical size of $\sim 1 \mu\text{m}$ but where no light contrast surface, indicative of bare gold, is visible. On the contrary, the barklike structure of the film can be seen all over the electrode surface down to its very end. This points to the importance, for a clean exposure of the tip end, of the bottleneck-shaped base on which the structures formed by the electric arc appear to systematically sit (see Figure 3). The exposure of the preformed structure may be facilitated by a pronounced electrostatic point effect at the edge of the neck. Alternatively, the neck may influence the way the paint spreads

(26) Oldham K. B. In *Microelectrodes: Theory and Applications*; Montenegro, M. I., Queiros, M. A., Daschbach, J. L., Eds.; NATO ASI Series E; Kluwer: Boston, 1991; Vol. 197, pp 35–50.

(27) Zoski, C. G.; Mirkin, M. V. *Anal. Chem.* **2002**, *74*, 1986–1992.

(28) Oatley, C. W. In *The Scanning Electron Microscope*; Cambridge University Press: London, 1972; Part 1, pp 174–175.

when heat-cured (see above), resulting in a thin and easy to remove film covering the preformed tip end.

Quantitative Characterization of the Submicrometer-Sized Spherical Electrodes by Cyclic Voltammetry. Having shown that the geometry of the submicroelectrodes is indeed as expected, their characterization by cyclic voltammetry can be accurately carried out. In particular, the voltametric characterization of the spherical microelectrodes can be refined as the theoretical response in cyclic voltammetry for microelectrodes of such geometry is known. The theoretical expression of the stationary voltammogram is, for a spherical microelectrode of radius a , given by eq 2:²⁶

$$i = \frac{4\pi FDC_p a}{1 + \exp(-\xi) + \exp(-\alpha\xi)/\Lambda} \quad (2)$$

with $\xi = (F/RT)(E - E_0)$ and $\Lambda = ak_s/D$. Λ is a kinetic parameter comparing the heterogeneous electron-transfer rate, characterized by the rate constant k_s , to the diffusion rate.

Taking for a the value given by the plateau current, the entire voltammogram can be fitted using expression 2 provided that k_s , D , and E^0 are known. To independently determine the value of these parameters, cyclic voltammetry experiments were conducted at conventional millimetric gold disk electrodes (data not shown). From the analysis of the reversible voltammogram obtained at low scan rates,²⁹ values of $D = 7.4 \times 10^{-6} \text{ cm}^2 \text{ s}^{-1}$ and $E^0 = 235 \text{ mV}$ versus SCE are determined. At higher scan rate, analysis of the voltammograms gives access³⁰ to a value of $k_s = 0.3 \pm 0.1 \text{ cm/s}$.

Using the above values of D and E^0 , the voltammograms presented in Figure 4c and d, which respectively correspond to spherical electrodes of a radius of 250 and 150 nm, can be satisfyingly fitted by eq 2 using a common value of k_s of 0.4 cm/s (open circles in Figure 4). This value compares favorably with the one determined at millimetric gold electrodes as described above. Moreover, the very fact that the value of k_s is, as it is supposed to be, independent of the electrode radius, is yet more evidence that the actual electrode surface is indeed the submicrometer-sized spherical structure preformed at the end of the gold wire.³

As can be seen in Figure 4, another interesting aspect of the cyclic voltammetry response recorded at the preformed microelectrodes is the lack of hysteresis between the forward and backward traces of the voltammograms. This indicates a low electrical capacity of the electrode that results from the good insulating properties of the reticulated cathodic electrophoretic paint. However, when the scan rate is raised to 10 V/s, a clear capacitive hysteresis appears on the voltammograms (data not shown), allowing one to measure a typical value for the electrode capacity of $\sim 5 \text{ pF}$. This capacity is clearly much higher than the one that can be expected from the double-layer capacity of the gold surface of the submicroelectrodes (a few tenths of pF). This indicates that the insulating film/solution interface acts as a capacitor. The overall capacity of the electrode is, however,

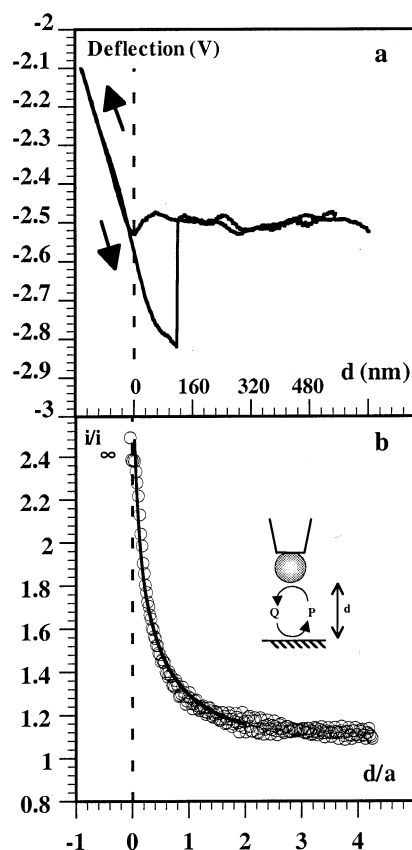


Figure 6. AFM/SECM experiment. A combined AFM/SECM spherical probe of radius $a = 155 \text{ nm}$ is approached from a conducting substrate. The variation of deflection as a function of the tip–substrate distance d is shown in (a) and the concomitant variation of the electrochemical current in (b). The positive feedback process is sketched in the inset in (b), P and Q respectively standing for ferrocenedimethanol and ferroceniumdimethanol. The solution contains 1 mM ferrocenedimethanol in 0.1 M KH_2PO_4 ; the probe is set at a potential where ferrocenedimethanol is oxidized at a diffusion-controlled rate (+0.3 V vs QRE). The gold conducting substrate is set at a potential where the reduction of the ferroceniumdimethanol, generated at the probe, is diffusion controlled (−0.15 V vs QRE). The approach speed is 100 nm/s. The current i is normalized by the value i_∞ it has at infinite tip–substrate separation. The current is not recorded during the retraction phase of the approach curve. The experimental electrochemical approach curves (open circles) are fitted by the theoretical curves (continuous line) calculated for a sphere cap electrode (see text). The hysteresis observed on the retracting part of the force curve (around $d = 0$) is due to the tip–substrate/gold–gold adhesion.

sufficiently low not to interfere with cyclic voltammetry measurements at scan rates up to a few volts per second.

Finally, it is also worth noting that the chemical stability of the coating is such that the potential window in aqueous solution in which the electrodes can be used without damaging the film is very large, ranging from about −1.2 to +1.7 V/SCE at pH 4.4. This contrasts with the much more fragile coating resulting from the anodic deposition of poly(acrylic acid)-based electrophoretic paints.¹²

Use of Submicrometer-Sized Spherical Electrodes as Combined AFM/SECM Gold Probes. The submicroelectrodes reported in the present work are converted into combined AFM/SECM probes following a published technique^{17a,b} that is only slightly modified as described in the Experimental Section.

(29) Andrieux, C. P.; Savéant, J.-M. In *Electrochemical Reactions in Investigation of Rates and Mechanisms of Reactions*, Techniques of Chemistry; Bernasconi, C. F., Ed.; Wiley: New York, 1986; Vol. VI/4E, Part 2, pp 305–390.

(30) Nicholson, R. S. *Anal. Chem.* **1965**, *37*, 1351–1355.

The combined AFM/SECM probe is then mounted at the extremity of the piezotube of a commercial AFM and immersed in a solution containing FcdiOH at 1 mM in 0.1 M KH_2PO_4 . The laser beam of the AFM is focused on the mirrorlike surface of the cantilever of the probe so that it is reflected toward the position-sensitive detector. The probe is set at a potential where FcdiOH oxidation is diffusion controlled (+0.3 V/QRE) and then lowered toward the substrate by the controlled elongation of the piezotube. The substrate, consisting of a flat gold surface, is set at a potential where the reduction of ferroceniumdimethanol, generated at the probe, is diffusion controlled (−0.15 V/QRE). During the approach, the position of the reflected laser beam onto the detector and the electrochemical current are simultaneously recorded as a function of the elongation of the piezotube and plotted as a deflection approach curve (Figure 6a) and a SECM approach curve (Figure 6b).

When the tip approaches from the substrate, a marked increase of the stationary current flowing through the probe is detected (see Figure 6b). This positive feedback arises when ferroceniumdimethanol molecules produced at the submicroelectrode are reduced at the substrate and fed back to the probe.¹

The sudden rise of the deflection signal observed during the approach results from the physical contact of the tip end with the surface and therefore defines the point of zero tip–surface separation ($d = 0$ in Figure 6). Due to the flexibility of the cantilever, such a physical contact between the probe and the surface occurs without damaging the preformed tip. However, the substrate potential being negative with respect to the one of the probe, the contact between the probe and the substrate results in an electrical short circuit. The occurrence of such short circuit incidentally shows that no remaining insulating film covers the surface of the very end of the submicroelectrode.

As can be seen, the experimental electrochemical approach curve recorded using a combined probe bearing a 155-nm-radius spherical electrode can be very satisfyingly fitted to the theoretical positive feedback curve calculated for a microsphere cap electrode.^{5b} Such a good fit would not have been possible had the actual geometry of the electrode not been spherical or had the tip presented electroactive areas other than the sphere. It also is interesting to note that a closest distance of approach before contact as small as $d/a = 0.05$, giving rise to a positive feedback

as high as $i/i_\infty = 2.5$, is attainable using the spherical submicrometer-sized electrode reported here as SECM probes (see Figure 6b). Such a close approach distance is an intrinsic benefit of the spherical shape of the electrode that is by nature insensitive to tip/substrate alignment errors. This contrasts with the situation met when disk-in-glass electrodes are used, as in this case, the large surrounding glass sheath often collides with the surface, thus severely limiting the approach.⁷ Protruding conical electrodes do not present such limitations; however, spherical electrodes result, for a same approach distance, in a much higher feedback.^{5,7a}

CONCLUSION

It has been demonstrated that submicrometer-sized electrodes of controllable geometry can be fabricated. The very end of an etched gold wire can be melted by a controlled arc discharge and modeled into microstructures, a few hundred of nanometers in size, of defined conical or spherical geometry. Deposition of cathodic electrophoretic paint onto the wire then results in a tight, reticulated, insulating film. The recurring problem of exposing *selectively* the preformed electrode, which implies removing the insulating film only at the very end of the tip, was solved in an original way by applying a high-voltage pulse to the insulated wire. Imaging by SEM, characterization by cyclic voltammetry, and metal deposition experiments converged to show that only the preformed spherical or conical tip end was indeed exposed. The resulting submicrometer-sized electrodes display good voltametric behavior and can be used as combined AFM/SECM probes of defined geometry.

ACKNOWLEDGMENT

The authors gratefully acknowledge Roland Ricard (BASF coatings) for the gift of the electrophoretic paint. Stephan Borensztajn (UPR 15 CNRS) is thanked for his help in obtaining the SEM images. Louis Pacheco (Scientec) is gratefully acknowledged for his help in setting up the AFM/SECM experiments. Financial support from the CNRS (Programme Nano-Objet Individuel 1999) is gratefully acknowledged.

Received for review June 10, 2002. Accepted October 1, 2002.

AC020385Z